Cryogenics 152 (2025) 104205

Contents lists available at ScienceDirect

Cryogenics

journal homepage: www.elsevier.com/locate/cryogenics

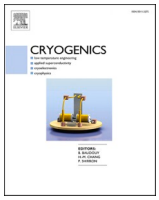

Hydrogen liquefaction by active magnetic regenerative refrigeration

Koji Kamiya [a,*], Kyohei Natsume [a], Akira Uchida [a], Takenori Numazawa [a], Tsuyoshi Shirai [a], Akiko T. Saito [a], Koichi Matsumoto [b], Shinji Masuyama [c]

[a] National Institute for Materials Science, 3-13 Sakura, Tsukuba, Ibaraki 305-0003 Japan
[b] Kanazawa University, Kakuma-machi, Kanazawa, Ishikawa 920-1192 Japan
[c] National Institute of Technology, Oshima College, Suo-oshima, Yamaguchi 742-2193 Japan

A B S T R A C T

Magnetic refrigeration is a cooling method that utilizes the magnetocaloric effect. The magnetocaloric effect induces temperature changes by varying the magnetic moment in response to changes in a magnetic field, eliminating the need for compression work as seen in conventional gas refrigerators. This enables high-efficiency cooling, making it suitable for cooling and liquefaction of cryogenic gases. In this study, we focused on an Active Magnetic Refrigeration (AMR) system, one of the magnetic refrigeration methods, capable of operating over a wide temperature range, and fabricated a dedicated AMR system for hydrogen liquefaction. The AMR developed in this study achieved a cooling power of 7.34 W and a relative Carnot efficiency of 60.5 %.

1. Introduction

Magnetic refrigeration utilizing magnetocaloric effect has been used for many years in ultra-low temperature research as a method to produce temperatures below 1 K, called Adiabatic Demagnetization Refrigerator (ADR) [1,2]. The first application of magnetic refrigeration to liquefy cryogenic gases was carried out by Nakagome et al. and Numazawa et al. [3,4]. Numazawa et al. used gadolinium gallium garnet as a magnetic refrigerant, and a superconducting magnet to produce a magnetic field of 3.1 T. They adopted a pulsed magnet system where both the magnetic refrigerant and the superconducting magnet remain stationary while inducing magnetic field changes by sweeping the current in the superconducting magnet. Based on the results of the refrigeration cycle, they reported a relative Carnot efficiency of 0.17.

Their system called Carnot Magnetic Refrigeration (CMR) is, however, based on the Carnot cycle utilizing only the magnetic entropy effect, which confines the operating temperature range to a few Kelvins. To achieve a broader operating temperature range, different approaches beyond the inherent material properties were necessary.

To address this issue, in 1984, Barclay proposed the Active Magnetic Regenerative Refrigeration (AMRR but we will refer to it as AMR), which involves utilizing a magnetic refrigerant not only for its magnetocaloric effects but also as a regenerator to expand the temperature range of magnetic refrigeration [5].

Switching attention to hydrogen, hydrogen liquefaction using the CMR by the pulsed magnet was first successfully achieved by Ohira et al. in the year 2000 [6]. They reported a Carnot efficiency of 37 % and the cooling power of 0.4 W. In 2006, Kamiya et al. achieved successful liquefaction of hydrogen by reciprocating CMR by physically moving a magnetic material in and out of a stationary magnetic field [7]. Subsequently, Yoshioka et al. reported that the cycle efficiency of the reciprocating CMR for hydrogen liquefaction was 37 % [8].

As of now, research and development on hydrogen liquefaction using AMR are primarily being carried out by Pacific Northwest National Laboratory (PNNL) in the United States [9], Korea Advanced Institute of Science and Technology (KAIST) in South Korea [10], and NIMS and Kanazawa University in Japan [11,12].

The AMR developed by PNNL plans to cover the temperature range from room temperature to liquid hydrogen temperature with reciprocating AMR with dual gadolinium. In 2019, they succeeded in liquefying propane at 218 K for the first time [13]. KAIST developed two-stage AMR for hydrogen liquefaction with liquid nitrogen pre-cooling. The feature of their device is that it is not reciprocating AMR but a pulsed magnet AMR as Numazawa et al. employed in their helium liquefaction. The AMR system developed by NIMS and Kanazawa University for hydrogen liquefaction is the magnetic refrigeration developed by NIMS employs the reciprocating driving of magnetic refrigerants and incorporates a pre-cooling GM cryocooler to control the heat rejection temperature of the AMR. In 2022, NIMS and Kanazawa University succeeded in liquefying hydrogen using this liquefier and their achievement was reported [14].

In this study, we report the details of the AMR hydrogen liquefaction

* Corresponding author.
E-mail address: kamiya.koji@nims.go.jp (K. Kamiya).

https://doi.org/10.1016/j.cryogenics.2025.104205
Received 19 July 2025; Received in revised form 9 September 2025; Accepted 26 September 2025
Available online 28 September 2025

experiment and discuss its cooling power and efficiency.

2. AMR cycle for hydrogen liquefaction

In this study, a tandem AMR configuration was adopted by connecting two AMR cylinders: upper AMR and lower AMR in series, as shown in Fig. 1. To enable the operation of both AMRs using a single heat exchange gas, they are driven in opposite phases to each other. The cycle of our AMR consists of the following 4 processes: (1) Magnetize the upper AMR and demagnetize the lower AMR, (2) Blow upward flow, (3) Magnetize the lower AMR and demagnetize the upper AMR, and (4) Blow downward flow. In process (1), the upper AMR warms up by magnetization, while the lower AMR is cooled by demagnetization. In process (2), by blowing the heat exchange gas upward, excess heat from the upper AMR is pushed outward and expel to the external upper region of the upper AMR. As for the lower AMR, the cooling power generated during demagnetization is pushed upward to cool the refrigerated objects placed between the upper and lower AMRs. Process (3) is the reverse of process (1), where the lower AMR is heated by magnetization, and the upper AMR is cooled by demagnetization. In process (4), downward flow pushes the excess heat from the lower AMR outward expel to the external lower region of the lower AMR. By repeating these four processes, the region between the upper and lower AMRs always remains at the cold temperature, making it possible to utilize it for cooling and liquefying hydrogen stably.

Fig. 2 shows a graph of some known magnetocaloric materials as a function of temperature [15]. While other promising materials such as HoB_2 and GdCoC have also been discovered [16–20], the well-characterized magnetocaloric materials are selected in Fig. 2. In this study, $HoAl_2$, a second-order phase transition material, was employed from among the materials shown in Fig. 2 because $HoAl_2$ covers the range around 20 K (the hydrogen liquefaction temperature) at 1 bar and 30 K (the heat dumping temperature). To avoid hydrogen embrittlement of $HoAl_2$ in this system, helium gas was used as the process gas instead of hydrogen.

3. Experimental set-up

Fig. 3 shows a picture and the internal schematic of the tandem AMR system introduced in Fig. 1 with enlargement of the AMR cylinders and a picture of $HoAl_2$ stamped particles. The AMRs are connected to an

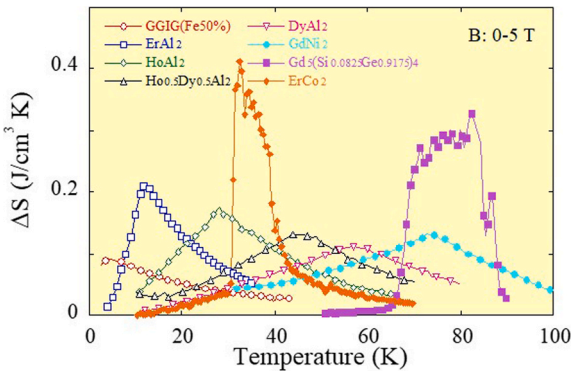

Fig. 2. A graph of the entropy changes of magnetocaloric materials as a function of temperature.

actuator (Intelligent Actuator, Inc., type RCS2- RA13R) outside the cryostat, and the actuator drives the AMRs by moving them up and down. As a heat exchange gas, about 1.7 MPa helium is used in this study. The reciprocating flow required by AMRs is generated using a compressor and 4 electromagnetic valves installed at room temperature. Heat input from room temperature is first reduced using a regenerative heat exchanger (RHX), then sufficiently pre-cooled through a mechanical cryocooler (Sumitomo Heavy Industries, Ltd type RDK-500B) via a conventional coil-type thermal anchor (AMR HX). The exhaust heat from the warm ends of the AMRs is also removed by the same mechanical cryocooler.

3.1. Helium gas circulation unit for reciprocating flow

Since the AMR needs reciprocating flow to operate the AMR cycle, it is essential to control the flow utilizing a simple displacer or a flow control device composed of a compressor and 4 electric valves (EV). Fig. 4 shows a diagram for a valve system of the AMR. Firstly, a compressor (ULVAC CRYOGENICS helium compressor unit SW115) supplies a unidirectional flow continuously. When a downward (clockwise) flow is required for the AMRs, EV1 and EV3 are opened while EV2 and EV4 are closed. Conversely, to create an upward flow, EV1 and EV3 are closed, and EV2 and EV4 are opened. The valve system in this study

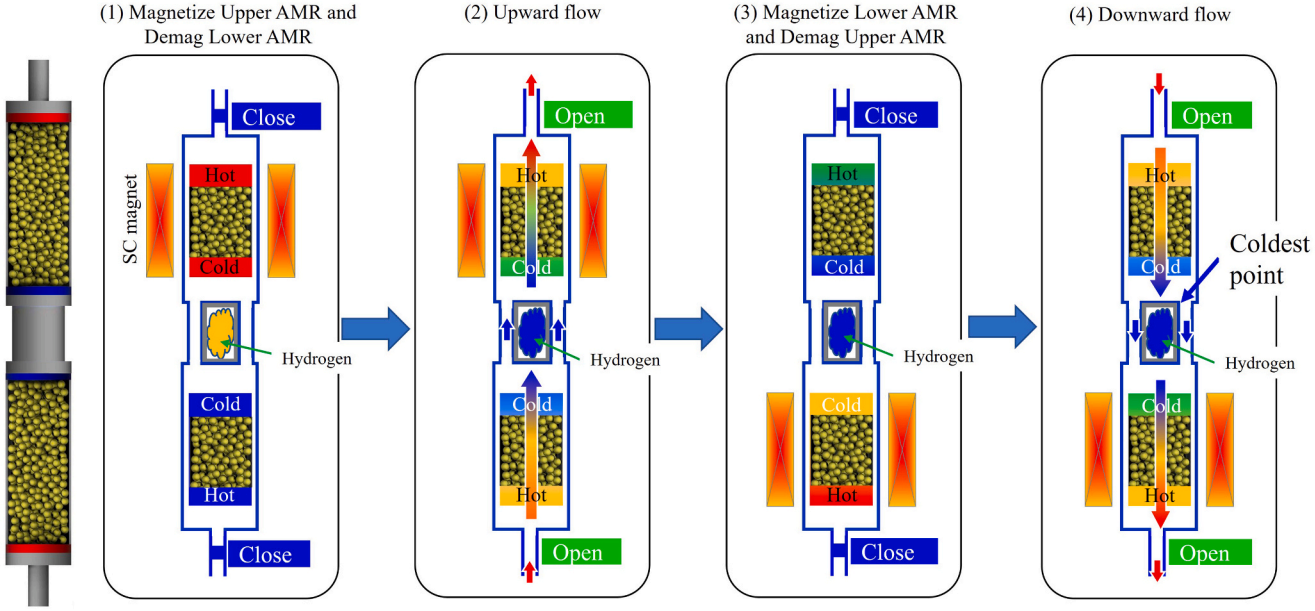

Fig. 1. Tandem AMR cycle for hydrogen liquefaction consists of 4 processes.

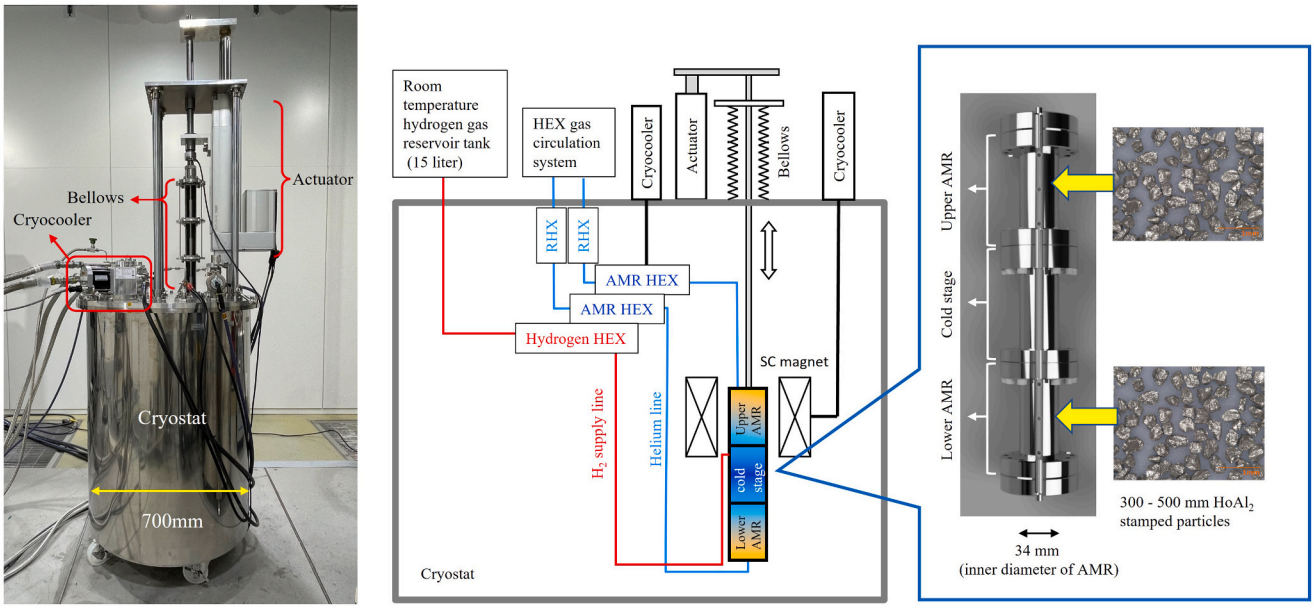

Fig. 3. Picture and schematic of AMR system for hydrogen liquefaction.

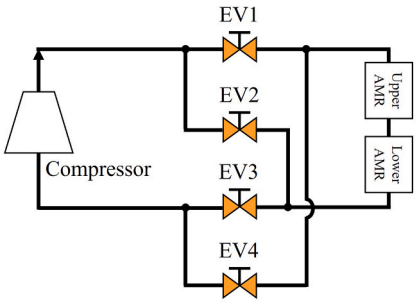

Fig. 4. The helium gas circulation unit to create reciprocating flow for the AMRs.

can control the timing and duration of valve openings.

3.2. Regenerative heat exchanger

To avoid an excessively large size of heat exchangers, the AMR heat exchanger adopts a compact regenerative type instead of the conventional type. This newly developed regenerative heat exchanger is integrated into the AMR system. Fig. 5 is a picture of newly developed regenerative heat exchanger, RHX as shown in Fig. 3. The RHX cylinder shape was determined using "REGEN3.3", a program that models heat transfer in regenerators developed at NIST [21]. According to REGEN, it was found that two sets of RHX with a length of 100 mm and an inner diameter of 25.4 mm are needed, in which 1800 sheets of #200 stainless steel meshes are stacked.

3.3. Superconducting magnet

The AMR system must need to use magnetic field. There two options: one is using permanent magnets, and the other is using superconducting magnets. Permanent magnets do not require a power supply, so the system becomes highly efficient. However, they are not suitable for applications requiring high cooling power due to their low magnetic field. For applications such as liquefaction that demand high cooling power, superconducting magnets are commonly used.

Fig. 6 shows the superconducting magnet used in this study, with a bore of 120 mm and a height of 300 mm, and a central magnetic field of 5 T. The magnet is cooled by a cryocooler at 4 K (RDE-412D4 manufactured by Sumitomo Heavy Industries, Ltd.). In this study, the AMR system generates magnetic field variations by moving the magnetic material vertically inside the superconducting magnet.

However, with a simple solenoid magnet alone, to achieve sufficiently low magnetic fields of less than 0.1 T, the magnetic material would need to be moved 700 mm from the center of the magnet. Therefore, in this study, we fabricated a magnet system where opposing magnetic fields are generated above and below the main magnet to actively shield the main magnetic field, resulting in a sharp decrease in the magnetic field outside the main magnet. Fig. 7 shows calculated spatial distributions of the magnetic field induced with only the main

Fig. 5. A picture of Regenerative Heat Exchanger (RHX) developed in this study.

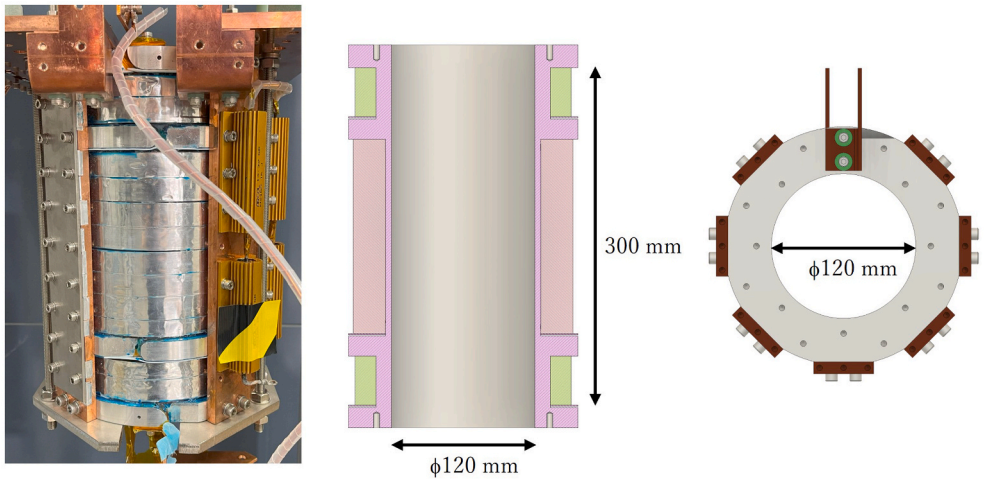

Fig. 6. A picture of the superconducting magnet developed for this study.

NbTi wire specification	
Manufacturer and model	SuperCon 54S43
Bare diameter	0.5 mm
Insulated diameter	0.54 mm
Cu: NbTi ratio	1.3:1

Main magnet design parameter	
Inner diameter	130 mm
Outer diameter	184 mm
Length	162 mm
Inductance	25.4 H

Sub magnet design parameter	
Inner diameter	146 mm
Outer diameter	181 mm
Length	41 mm
Inductance	2.9 H

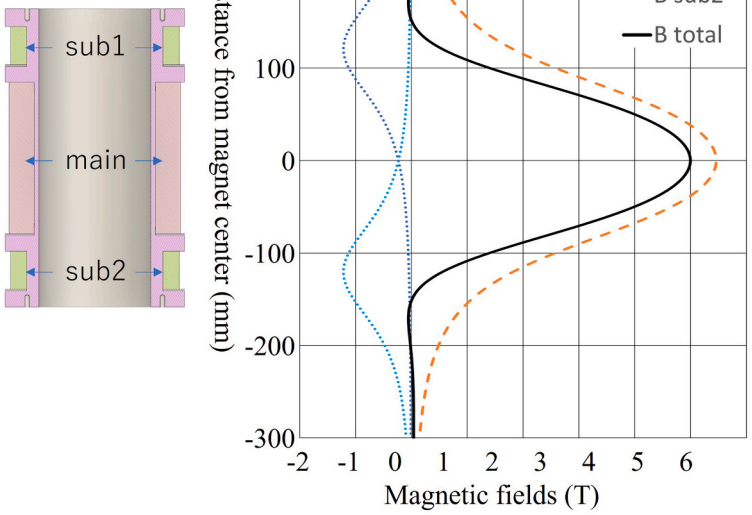

Fig. 7. Specification of NbTi wires and magnets (left) and calculated spatial distribution of the magnetic field with and without sub magnets (right).

magnet together with the sub magnets with specification of the superconducting wire and the magnet system. By using this magnet, the required movement distance of the magnetic material was reduced to 200 mm. Fig. 8 is a comparison between calculation and measurement of the field, and it is evident that both closely match.

In the experiment, the mass flow rate and magnetic field are provided as shown in Fig. 9 to realize the AMR cycle depicted in Fig. 1.

3.4. Hydrogen vessel and level sensor

The hydrogen vessel is located within the region called the "Cold Stage" between the upper and lower AMRs as shown in Fig. 10. Helium flows through the Cold Stage, carrying the cold helium gas. Additionally, a separate vessel called the hydrogen vessel is installed within the Cold Stage to store liquid hydrogen. The hydrogen vessel has multiple notched fins to efficiently transmit the cooling power from helium of the AMR to the hydrogen vessel [22].

Initially, hydrogen gas is introduced inside the hydrogen vessel, and through the AMR process, hydrogen gas in the vessel is gradually cooled and eventually liquefied. The liquid hydrogen is detected using a liquid level sensor. Since the hydrogen vessel is very small (inner diameter of 10 mm), commercially available liquid level sensors cannot be used. Therefore, in this study, three custom-made small liquid level sensors using silicon diodes were utilized for detecting liquid hydrogen [23]. The silicon diode is operated with a current higher than its rated value to overheat. Due to the difference in heat transfer rates, the output of the sensor varies when it is in contact with hydrogen gas compared to when it is in contact with liquid hydrogen.

4. Hydrogen liquefaction experiment with AMR

Fig. 11 is an example of liquefaction experimental results. Fig. 11 consists of 2 graphs. The upper graph represents the temperature variation in the AMR, while the lower graph represents the output of the liquid level sensors. The conditions of the experiment in Fig. 11 are magnetic field of 5 Tesla, AMR cylinder speed of 50 mm/sec, helium gas

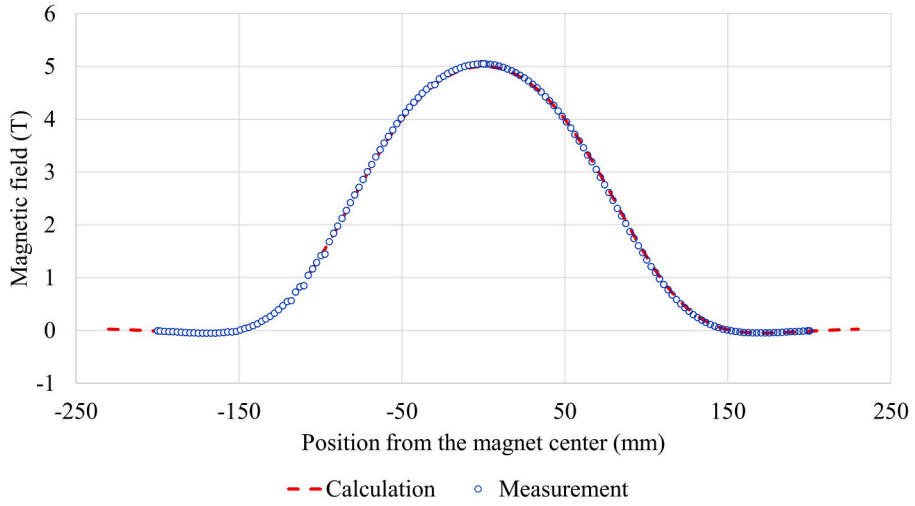

Fig. 8. Comparison of the magnetic field between calculation and measurement.

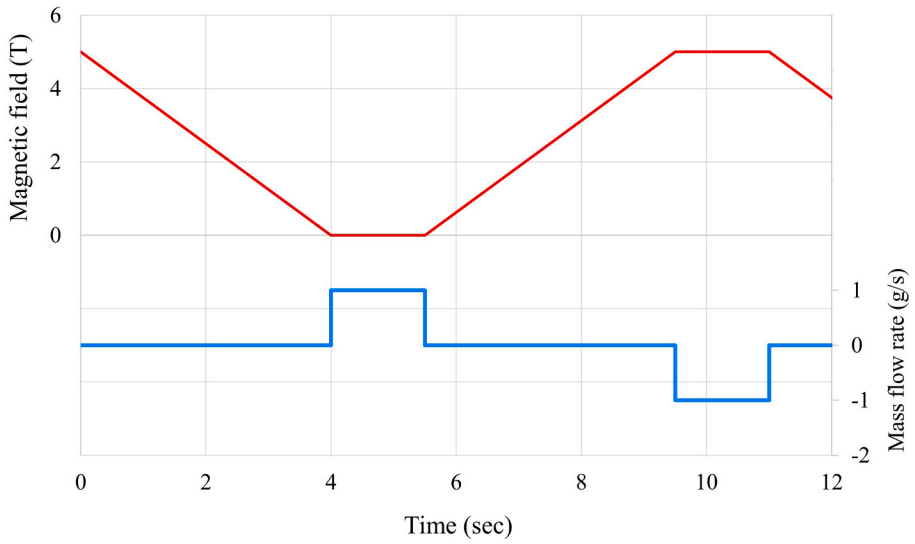

Fig. 9. Schematic operation conditions of magnetic field variation and mass flow rate.

average pressure of 1.1 MPa, and hydrogen pressure of 0.1 MPa.

As the experiment begins, the hot end temperature of the AMR cylinder increases, while the cold end temperature decreases, eventually reaching a temperature difference of about 12 K in average between the hot end and the cold end. Meanwhile, it can be observed that the temperature of the Cold Stage is continuously decreasing.

4.1. Hydrogen liquefaction with the AMR

The outputs of the liquid level sensors are shown in the lower graph in Fig. 11. The output voltage has been increasing from the beginning of the experiment. The output of the silicon-diode increases with the decrease in temperature, indicating that the hydrogen gas is cooling down. Due to the magnetic field dependency of the silicon iron, its output varies with the magnetization and demagnetization. However, the output variations caused by cooling exceed the variations due to the magnetic field, making it suitable for use as a liquid level sensor. Since the hydrogen is in a gaseous state at the beginning of cooling, all three liquid level sensors are uniformly getting colder. However, as the liquefaction process begins and liquid storage commences, the liquid level eventually reaches the lower-level sensor. Due to the different heat transfer coefficient between gas and liquid, the temperature of the overheated level sensors in contact with the liquid appears to further decrease. The liquid hydrogen level continuously rises and encounters the middle and upper-level sensors.

4.2. Cooling power and efficiency of AMR

The cooling power of the AMR in Fig. 11, which successfully demonstrated hydrogen liquefaction, is about 3 W. Subsequently we attempted to further improve the cooling power by increasing the mass flow rate of the heat exchange gas. For this purpose, a SW115 manufactured by ULVAC cryogenics inc. with a rated power of 2 kW and mass flow rate of approximately 1 g/s was replaced with a CSW-71 by Sumitomo Heavy Industries, Ltd. with a rated power of 7 kW and mass flow rate of approximately 4 g/s, and hydrogen liquefaction by the AMR cycle was conducted.

The cooling power of the AMR in this study was measured as follows:

(1) When AMR starts, the hydrogen liquid level rises in the hydrogen liquefaction layer.

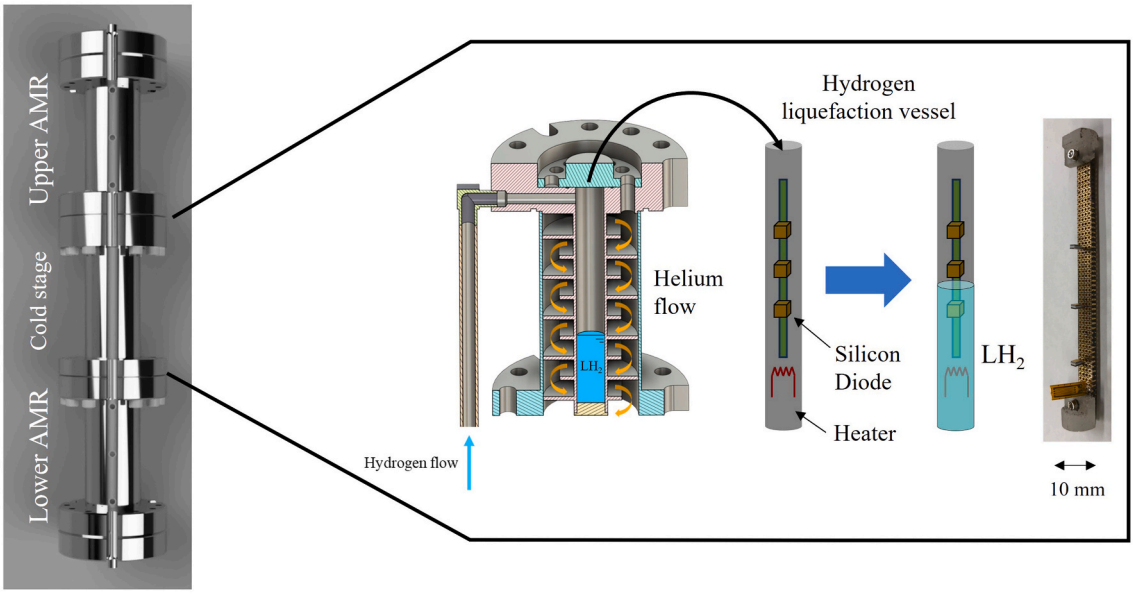

Fig. 10. Hydrogen vessel with notched fins and liquid hydrogen level sensor.

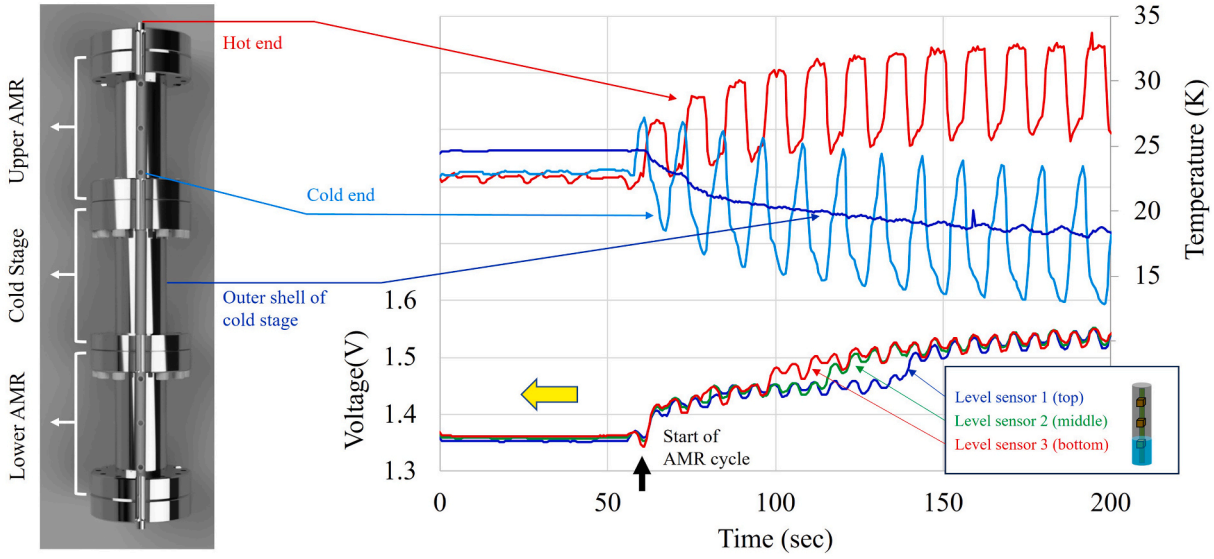

Fig. 11. An example of hydrogen liquefaction experiment by the AMR system.

(2) The heater is controlled so that the liquid level stays between the level sensors 1 and 2 as shown in Fig. 12.

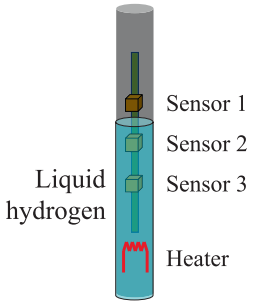

Fig. 12. A liquid hydrogen vessel and level control using sensors 1 and 2 (Silicon Diode), and a heater.

(3) The heater output at that time is equal to the cooling power of the AMR.

In this study, the cooling power obtained by the above procedure was measured as a function of the cycle time of one cycle, varying only the speed at which the magnetic material was driven. The results are slotted in Fig. 13. In general, the cooling power increases with shorter cycle time, but Fig. 13 shows that this is not true when the cycle time is less than 6.6 s, with a maximum value of 7.34 W. The reason for this is that the inefficiency of the heat exchange between the magnetic material and the heat exchange gas exceeds the increase in cooling power when the cycle time is less than 6.6 s.

4.3. *Efficiency of AMR*

In order to determine the efficiency of the AMR, an AMR cycle in the temperature-entropy diagram during hydrogen liquefaction was plotted as shown in Fig. 14. In Fig. 14, Temperature-Entropy (T-S) diagrams at

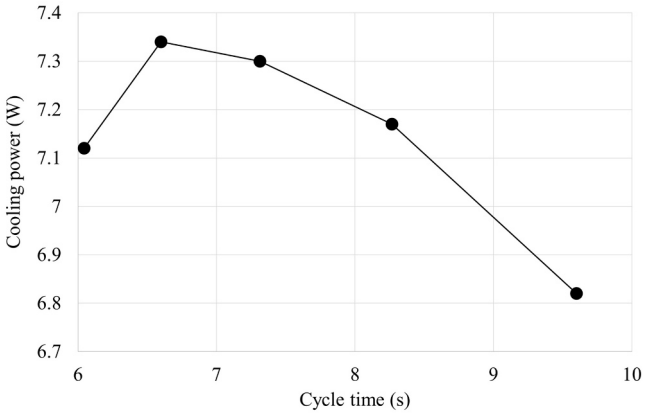

Fig. 13. Cooling power as a function of cycle time.

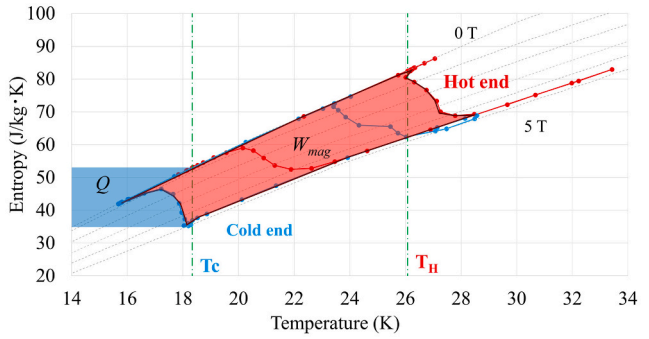

Fig. 14. The temperature and entropy (T-S) diagram of AMR during liquefaction. The cooling capacity Q and input work W_{mag} for efficiency calculation are shown.

the hot end and the cold end of the lower AMR are plotted.

In the TS diagram, T_c is defined as the temperature at the end of the demagnetization process at the cold end, and T_H is defined as the temperature at the end of the magnetization process at the hot end. Therefore, the cooling capacity is represented by the area (Q) enclosed in blue. It should be noted that, although not fully illustrated in Fig. 14, the blue region in fact extends down to 0 K. Similarly, the input work is given by the area (W_{mag}) enclosed in red.

In addition to W_{mag}, there is the pump work W_{pump} required to drive the heat exchange fluid in the AMR. Calculating W_{pump} using Ergun's equation [24] for fluid pressure loss in a particle-filled pipe yields the following coefficient of performance (COP) for the AMR as below:

$$COP_{AMR} = \frac{Q}{W_{mag} + W_{pump}} \tag{3}$$

Using the ideal (Carnot) COP calculated from T_c and T_H, the relative Carnot efficiency η is obtained as below:

$$\eta = \frac{COP_{AMR}}{COP_{Carnot}} \tag{4}$$

From Eq. (4), the relative Carnot efficiency of the lower AMR was found to be 66.5 %.

The same calculation was performed for the upper AMR, and the result was found to be 54.4 %, resulting in an overall efficiency of 60.5 %, which is the average of the efficiencies of the upper and lower AMRs obtained from the T-S diagram.

5. Summary

In this study, an AMR dedicated for hydrogen liquefaction was developed as follows:

(1) The AMR system is designed as a tandem AMR system consisting of two AMRs (upper and lower AMRs), so that the two AMRs are driven by a single heat exchange gas.
(2) A gas circulation system was fabricated and introduced to generate the reciprocating heat exchange gas necessary for the AMR.
(3) Regenerative heat exchangers were installed to reduce the heat input from the ambient temperature gas supplied by the circulation system in as small a space as possible.
(4) A superconducting magnet with a compensation coil was fabricated to minimize the driving distance of the AMR.

The AMR cycle was demonstrated in the assembled system and was found to successfully liquefy hydrogen, with a cooling power of 7.34 W and a relative Carnot efficiency of 60.5 % on the T-S diagram.

This work was supported by the JST-Mirai Program Grant Number JPMJMI18A3, Japan.

CRediT authorship contribution statement

Koji Kamiya: Writing – original draft, Validation, Methodology, Investigation, Data curation. **Kyohei Natsume:** Project administration, Methodology, Formal analysis, Data curation. **Akira Uchida:** Validation, Software, Methodology, Investigation, Formal analysis, Data curation. **Takenori Numazawa:** Supervision, Project administration, Funding acquisition, Conceptualization. **Tsuyoshi Shirai:** Validation, Methodology, Investigation, Formal analysis, Data curation. **Akiko T. Saito:** Resources, Investigation. **Koichi Matsumoto:** Writing – review & editing, Writing – original draft, Validation, Supervision, Investigation, Formal analysis, Data curation. **Shinji Masuyama:** Writing – review & editing, Writing – original draft, Resources, Investigation.

Declaration of competing interest

The authors declare that they have no known competing financial interests or personal relationships that could have appeared to influence the work reported in this paper.

Data availability

No data was used for the research described in the article.

References

[1] Giauque WF. A thermodynamic treatment of certain magnetic effects. a proposed method of producing temperatures considerably below 1° absolute. J. American Chem Soc 1927;49:1864.
[2] Giauque WF, MacDougall DP. Attainment of Temperatures Below 1° absolute by Demagnetization of $Gd_2(SO_4)_3 \cdot 8H_2O$. Phys Rev 1933;43:768.
[3] Nakagome H, Tanji N, Horigami O, Ogiwara H, Numazawa T, Watanabe Y, et al. The Helium magnetic Refrigerator I: Development and Experimental results. Adv Cryog Eng 1984;29:581.
[4] Numazawa T, Hashimoto T, Nakagome H, Tanji N, Horigome O. The Helium magnetic Refrigerator II: Liquefaction Process and Efficiency. Adv Cryog Eng 1984; 29:589.
[5] Barclay JA, Steyert WA. Active magnetic regenerator. U.S. Patent 4,332 1982; 135.
[6] Ohira K, Nakamichi K, Furumoto H. Experimental study on magnetic refrigeration for the liquefaction of hydrogen. Adv Cryog Eng 2000;45:1747.
[7] Kamiya K, Takahashi H, Numazawa T, Nozawa H, Yanagitani T. Cryocoolers 2007; 14:637.
[8] Yoshioka S, Kamiya K, Numazawa T, Nakagome H, Fukamichi K, Fujita A, Fujieda S, Nozawa H, Yanagitani T. Development of magnetic refrigerator for hydrogen liquefaction -Experimental results 3-. In: Proceedings of 76th Conference on Cryogenics and Superconductivity Society of Japan, Chiba, Japan; 2007. p. 138.
[9] Holladay JD, Teyber RP, Meinhardt KD, Polikarpov E, Thomsen EC, Archipley C, et al. Investigation of bypass fluid flow in an active magnetic regenerative liquefier. Cryogenics 2018;93:34.
[10] Kim Y, Park I, Jeong S. Experimental investigation of two-stage active magnetic regenerative refrigerator operating between 77 K and 20 K. Cryogenics 2013;57: 113.

[11] Matsumoto K, Kondo T, Yoshioka S, Kamiya K, Numazawa T. J Phys Conf Ser 2009; 150:12028.
[12] Numazawa T, Kamiya K, Utaki U, Matsumoto K. Magnetic refrigeration for hydrogen liquefaction. Cryogenics 2014;62:185–92.
[13] Barclay J, Brooks K, Cui J, Holladay J, Meinhardt K, Polikarpov E. and Edwin Thomsen. J Propane liquefaction with an active magnetic regenerative liquefier, Cryogenics 2019;100:69–76.
[14] Kamiya K, Matsumoto K, Numazawa T, Masuyama S, Takeya H, Saito AT, et al. Active magnetic regenerative refrigeration using superconducting solenoid for hydrogen liquefaction. Appl Phys Exp 2022;15:063001.
[15] K. Matsumoto, Private Communication.
[16] Castro PBD, Terashima K, Yamamoto TD, et al. Machine-learning-guided discovery of the gigantic magnetocaloric effect in HoB_2 near the hydrogen liquefaction temperature. NPG Asia Mater 2020;12:35.
[17] Zexuan Wang AM, Döring OV, Xin Tang KP, Skokov N, Terada T, Ohkubo O, et al. Enhanced mechanical performance of HoB2-based compounds without sacrificing cryogenic magnetocaloric effects. Acta Materialia 2025;296:121227.
[18] Zhang Y, Hao W, Shen J, Mo Z, Gottschall T, Li L. Investigation of the structural and magnetic properties of the GdCoC compound featuring excellent cryogenic magnetocaloric performance. Acta Materialia 2024;276:120128.
[19] Zhang Y, Na Y, Xie Y, Zhao X. Unveiling the structural and magnetic properties of $RENaGeO_4$ (RE = Gd, Dy, and Ho) oxides and remarkable low-temperature magnetocaloric responses in GdNaGeO4 oxide. J Mater Chem A 2025;13: 19923–32.
[20] Ćwik J, Koshkid'ko Y, Shinde K, Park J, Antunes de Oliveira N, Babij M, Czernuszewicz A. Magnetic and magnetocaloric properties of Dy1-xErxNi2 solid solutions and their promise for hydrogen liquefaction. J Mater Chem C 2024;12: 14421–32.
[21] Gary J. About the REGEN3.2 and REGEN3.3 Packages, http://math.nist.gov/archive/regen/.
[22] Fietz WH, Heller R, Kienzler A, Lietzow R. High temperature superconductor current leads for WENDELSTEIN 7-X and JT-60SA. IEEE Transactions on Applied Superconductivity 2009;19:2202.
[23] Dempsey PJ, Fabik RH. NASA Technical Memorandum 105541 Prepared for the 38th International Instrumentation Symposium, Apr 26-30. 1992.
[24] S. Ergun Fluid Flow through Packed Columns Chem Eng Prog 48 1952 89 94.